Surface & Coatings Technology 205 (2010) 1350–1355

Contents lists available at ScienceDirect

Surface & Coatings Technology

journal homepage: www.elsevier.com/locate/surfcoat

Control of lubricant transport by a CrN diffusion barrier layer during high-temperature sliding of a CrN–Ag composite coating

C.P. Mulligan [a,c,*], T.A. Blanchet [b], D. Gall [a]

[a] Department of Materials Science and Engineering, Rensselaer Polytechnic Institute, Troy, NY 12180, United States
[b] Department of Mechanical, Aerospace, and Nuclear Engineering, Rensselaer Polytechnic Institute, Troy, NY 12180, United States
[c] Benet Laboratories, U.S. Army Armament Research Development & Engineering Center, Watervliet, NY 12189, United States

ARTICLE INFO

Available online 4 August 2010

Keywords:
CrN–Ag
Nanocomposite coating
Solid lubrication
High-temperature materials
Sliding wear
Diffusion barrier

ABSTRACT

CrN–Ag composite coatings, 2 and 5 μm thick and containing 22 at.% Ag solid lubricant, were grown on Si(001) and 440C stainless steel substrates by reactive co-sputtering at $T_s = 500$ °C, and were covered with 200 nm thick pure CrN diffusion barrier cap layers. Annealing experiments at $T_a = 625$ °C, followed by quantitative scanning electron microscopy, energy dispersive x-ray spectroscopy, and Auger depth profile analyses indicate considerable Ag transport to the top surface for a barrier layer deposited at a substrate floating potential of −30 V, but negligible Ag diffusion when deposited with a substrate bias potential of −150 V. This is attributed to ion-irradiation induced densification which makes the cap layer an effective diffusion barrier. High temperature tribological sliding tests of this coating system against alumina balls at $T_t = 550$ °C indicate an initial friction coefficient $\mu = 0.43 \pm 0.04$ which decreases monotonically to 0.23 ± 0.03. This is attributed to the development of wear mediated openings in the barrier layer which allow Ag lubricant to diffuse to the sliding top surface. In contrast, pure CrN exhibits a constant $\mu = 0.41 \pm 0.02$ while CrN–Ag composite coatings without cap layer show a low transient $\mu = 0.16 \pm 0.03$, attributed to Ag transport to the surface, that however increases to $\mu = 0.39 \pm 0.04$ after ~6000 cycles as the Ag reservoir in the coating is depleted. That is, the dense CrN cap layer reduces the Ag lubricant flow rate and therefore prolongs the time when the coating provides effective lubrication. This results in a cumulative wear rate over 10,000 cycles of 3.1×10^{-6} mm^3/Nm, which is 3.3× lower than without diffusion barrier layer.

Published by Elsevier B.V.

1. Introduction

Self-lubricating composite and multilayer films providing solid lubrication have been a subject of interest for a number of years. Among these various composites or multilayers are those which combine a hard matrix phase to provide wear resistance with different soft lubricious phases that provide a lubricious bearing layer at ambient and elevated temperatures as well as in a variety of aggressive environments, as discussed in the comprehensive review papers given in references [1–5]. Applications for these enabling materials range from advanced turbomachinery and aerospace devices [6–9] to dry high-speed cutting and machining operations [10] to elimination of conventional lubricants in weapon action components [11]. Many of the composites contain solid lubricating materials such as Ag that diffuse to the surface during operation to provide reduced friction over long operating periods [12–23]. Prior studies on Ag-containing oxide [12,18–20] and nitride [13–15,17] coatings have shown that elevated temperature leads to Ag diffusion to the surface, yielding a lubricious bearing layer. As many studies have pointed out, it can however be a challenge to adequately control the lubricant transport rate to allow for low friction and wear over the long-term [13–17]. We have recently shown for CrN–Ag nanocomposites grown by reactive magnetron sputtering that Ag segregates from the CrN matrix to form a composite with aggregates increasing in size from $<10^5$, to 9×10^6 to 7×10^7 nm^3 for growth temperatures $T_s = 500$, 600, and 700 °C, respectively [13,24]. This change in aggregate size causes an associated change in the temperature at which lubricant transport is activated and also affects the transport rate itself [13]. Therefore, using microstructural changes due to changes in T_s, the tribological response can be optimized by designing coatings with transport rates most suitable for a given operating temperature, load, contact velocity, etc. In order to optimize the tribological performance of these coatings further, in particular at temperatures above the temperature activated lubricant transport point, we envision to use a dense barrier layer which initially encapsulates the solid lubricant within the matrix and prevents fast depletion of the lubricant which, in turn, prolongs the coating lifetime. This approach is motivated by reported studies that successfully

* Corresponding author. 1 Buffington St., Benet Laboratories, Bldg. 115, RDAR-WSB-LB, Watervliet, NY 12189-4000, United States. Tel.: +1 518 266 5415; fax: +1 518 266 5161.
E-mail address: c.mulligan@us.army.mil (C.P. Mulligan).

0257-8972/$ – see front matter. Published by Elsevier B.V.
doi:10.1016/j.surfcoat.2010.07.071

employed diffusion barriers and multi-layer structures [12,16] to engineer the high-temperature tribological response.

In this manuscript, we demonstrate the effectiveness of a dense pure CrN cap layer as a diffusion barrier to control Ag diffusion to the surface of CrN–Ag composite coatings, and also present the resulting tribological response. CrN is expected to be an effective diffusion barrier for Ag, due to the negligible Ag solubility in CrN, as long as it exhibits a dense microstructure. The dense microstructure is achieved in the present study by the use of ion-irradiation during growth, which is known to yield dense microstructures for various materials systems [25–27], and has also been reported to be effective for the case of epitaxial CrN layers [28]. Additionally, the continuous nature of the deposition from the CrN–Ag composite transitioning to the CrN cap layer without any post-processing or need for additional target materials is simple and scalable, making it very promising in terms of the overall manufacturability of this model coating system.

2. Experimental procedure

All coatings were grown in a load-locked multi-chamber ultra-high vacuum (UHV) stainless steel dc dual magnetron sputter deposition system with a base pressure of 1.3×10^{-7} Pa. Water cooled 5 cm diameter Cr and Ag targets with purities of 99.95% and 99.99%, respectively, were positioned at 10.5 and 21.6 cm from the substrate at an angle of 45° with respect to the substrate surface normal. The substrates, Si(001) wafers as well as 5 mm thick and 19 mm diameter metallographically polished 440C stainless steel disks (final polish with a 0.03 μm γ-alumina slurry), were cleaned with successive rinses in ultrasonic baths of trichloroethane, acetone, and isopropanol and blown dry with dry N_2. The substrates were mounted on a molybdenum holder using Pelco colloidal silver paste and inserted into the load-lock chamber for transport to the deposition chamber where they were heated with a resistive heater to the desired growth temperature $T_s = 500$ °C. Pure N_2 (99.999%) was further purified using a Micro Torr purifier and introduced through metering valves to reach a constant chamber pressure of 0.4 Pa, which was measured using a capacitance manometer. A total of four coating architectures were deposited: (1) pure CrN, (2) CrN–Ag, (3) CrN–Ag with a 200 nm pure CrN cap layer, and (4) CrN–Ag with a 200 nm pure CrN cap layer deposited with d.c. substrate bias. A 200 nm cap layer was used to ensure sufficient thickness to provide for an effective diffusion barrier. Additionally, in relation to the expected wear rate, the cap layer thickness ensures that changes in tribological response related to penetration of the cap layer into the underlying composite will not be confused with run-in behavior. Just prior to initiating deposition, the targets were sputter cleaned for 5 min while the substrate was covered with a protective shutter. Sputtering was carried out at a constant power of 450 W to the Cr target for pure CrN deposition. For deposition of the composites, constant powers of 450 W and 160 W were applied to the Cr and Ag targets, respectively, yielding deposition rates of 30 nm/min for CrN and 15 nm/min for Ag, as determined from cross-sectional micrographs of pure CrN and Ag layers. During deposition, the substrates were at a floating potential of −30 V, as measured directly on the substrate, and were continuously rotated about the polar axis with 50 rpm, in order to obtain optimal coating uniformity to a coating thickness of 5 μm for steel substrates and 2 μm for Si substrates. For deposition of the 200 nm CrN cap layers, for architecture (3) the floating potential remained at −30 V while for architecture (4), the substrate bias was set to −150 V. The ion-to-metal flux ratio for the deposition of the cap layers is estimated to be 8:1, based on the measured current at the sample stage, the coating deposition rate, and the sample holder surface area. The plasma potential during the depositions is not known, but is expected to be close to 0 V, based on the relative electrode areas, so that the N_2^+-ion energies are assumed to be $E_i = 30$ and 150 eV, respectively. The deposition temperature, including the contribution due to plasma heating, was measured using a pyrometer which was cross-calibrated with a thermocouple within the sample stage.

Vacuum annealing experiments to study Ag lubricant transport to the surface for the composite coatings deposited on Si were completed in the above described deposition system at $T_a = 625$ °C for a time of 20 min, with a background pressure $< 1\times10^{-5}$ Pa. Structural and compositional analyses of the surfaces were completed using Scanning Electron Microscopy (SEM) and Energy Dispersive X-ray Spectroscopy (EDS), respectively, in a JEOL JSM-840A SEM with a Kevex Instruments model 2003 detector as well as a JEOL JSM-6330F FE-SEM. For EDS analyses, the e-beam voltage was reduced from 20 to 10 keV, in order to increase surface sensitivity.

The Ag concentration as a function of depth was determined by completing Auger depth profile measurements for coatings deposited on Si, using a PHI 600 scanning Auger microscope. Prior to any sputter cleaning, Auger survey scans were completed to determine the initial composition before any alterations in composition could occur from preferential sputtering due to differences in sputter yields of the elements. Sputtering was carried out with a 500 eV Ar^+ ion beam, yielding a sputter rate of ~15 nm/min. A 1 min sputter cleaning step to remove contamination from the surface was followed by depth profiling using 1 min sputter cycles, with spectra taken in between cycles with the sputter gun turned off.

High temperature tribological properties at $T_t = 550$ °C were measured by sliding 6 mm diameter alumina balls for 10,000 cycles using a Nanovea Series ball-on-disk tribometer in laboratory air (35–45% relative humidity at room temperature). A total sliding distance of 157 m was obtained using a 5-mm-diameter wear track and a sliding speed of 5 cm/s corresponding to 191 rpm. A normal load of 5 N was applied, yielding a calculated maximum Hertzian contact stress and initial Hertzian contact radius of 1.3 GPa and 0.04 mm, respectively. The hardness of the alumina counterface is 15 GPa at room temperature but decreases to 8.5 GPa at 500 °C [29]. Prior to initiating sliding, the samples were held for 30 min at the given testing temperature. Friction coefficients were recorded continuously throughout testing.

After tribological testing, the surfaces of the coatings were analyzed using a Nanovea ST400 non-contact optical profilometer. The total coating wear volume, as defined by the material loss below the initial sample surface, was determined using 3-D surface topography data from two segments of the wear track located 180° from each other. The two segments were 1 mm long and exhibited wear volumes and wear track widths that were uniform to each other within ±9% for all coatings. The reported wear rates are based on the wear volumes obtained from the average of the two segments, extrapolated over the entire circular track.

3. Results and discussion

3.1. Temperature activated lubricant transport

Fig. 1 shows plan view scanning electron micrographs of CrN–Ag composite coatings that were deposited on Si substrates at $T_s = 500$ °C and covered with a 200 nm thick pure CrN cap layer. The images along the top are from as-deposited surfaces where the cap layers were deposited at floating potential (left) and at −150 V bias (right), corresponding to ion energies of 30 and 150 eV, respectively, and directly below are from the same samples, however, after simultaneous annealing at $T_a = 625$ °C for 20 min. Both as-deposited surfaces are smooth, without any Ag agglomerates. In contrast, the coating deposited with cap layer grown at floating potential shows 8.3×10^5 mm^{-2} surface agglomerates that were identified by EDS elemental mapping (not shown) as Ag grains that appear in this micrograph as bright contrast, due to the higher secondary electron yield of Ag versus Cr. This Ag at the surface is attributed to Ag that diffuses during the annealing step from the CrN–Ag composite coating through the pure CrN cap layer to the

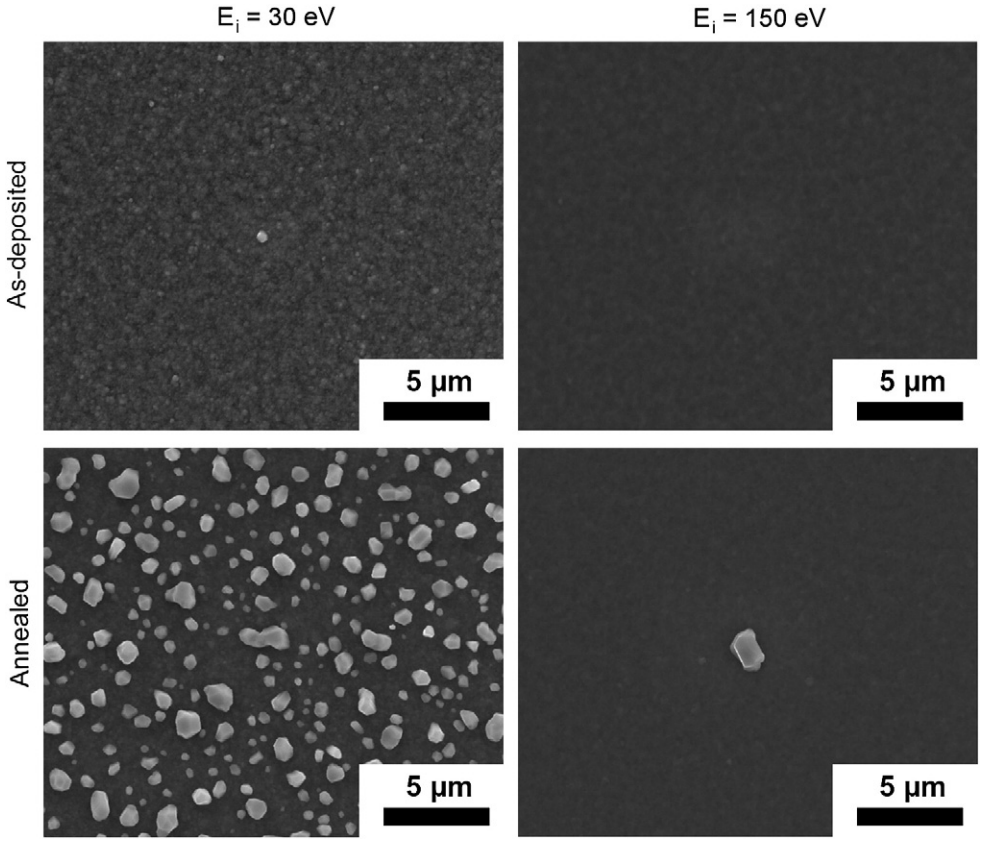

Fig. 1. Plan-view SEM micrographs of as-deposited CrN–Ag coatings covered with 200-nm-thick pure CrN cap layers deposited with an ion energy E_i of (left) 30 eV and (right) 150 eV. The micrographs below are from the same samples after annealing at $T_a = 625$ °C for 20 min.

open surface. Based on our previous studies [13,15,23], Ag is expected to be very mobile within the CrN–Ag coating since the annealing temperature is well above the growth temperature. In addition, the micrograph at left shows that Ag is also very mobile in the pure CrN cap layer grown with $E_i = 30$ eV during annealing at $T_a = 625$ °C. We attribute this to a porous columnar microstructure, as we have previously shown in Ref. 24. The annealed sample at right for the $E_i = 150$ eV sample, shows a single Ag surface grain. Large area analyses provide an estimate of the Ag grain density to be $< 10^2$ mm^{-2}, which is more than 3 orders of magnitude smaller than for the sample grown without bias. That is, the cap layer grown with −150 V bias effectively acts as a diffusion barrier against Ag lubricant transport. The dramatic difference between $E_i = 30$ and 150 eV is attributed to ion-irradiation induced densification as illustrated for CrN in prior work [28]. That is, 30 eV ion bombardment is not sufficient to suppress the formation of open pores between the growing CrN columns which are required for the insoluble Ag to diffuse to the surface, while 150 eV causes densification, resulting in dense CrN which acts as diffusion barrier. These results are consistent with previous studies on transition metal nitrides that reported the onset ion-irradiation energy for bulk displacement events to be around 50 eV [30,31].

The absence of any appreciable lubricant transport for the $E_i = 150$ eV sample is confirmed by Auger depth profile analyses shown in Fig. 2. The measured Ag concentration is plotted versus the entire coating thickness for the as-deposited and the annealed coating for the case of (a) CrN–Ag with dense CrN cap layer and (b) CrN–Ag without cap layer. In Fig. 2(a), the plots show a negligible Ag concentration in the pure CrN cap layer, 14 at.% in the CrN–Ag composite, and a drop towards 0% for the Si substrate. The apparent finite value in the cap of 2 at.% is an experimental artifact associated with the quantitative spectrum analysis, while the low Ag values of 14–15 at.% in the as-deposited condition for both Fig. 2(a) and (b) are attributed to differential sputter yields for the various elements [32]. The initial Auger survey spectra taken prior to any sputtering indicate a Ag content of 22 at.%, as expected from deposition rate calibrations, and a slightly understoichiometric CrN_x matrix with $x = 0.95$–0.98, when ignoring initial carbon, sulfur, and oxygen signals associated with surface contamination. The plots in Fig. 2(a) before and after annealing are identical within the measurement noise, confirming that essentially all Ag remains in the coating, consistent with the plan view micrograph for $E_i = 150$ eV following annealing in Fig. 1. This is contrary to Fig. 2(b) where the reduced Ag concentration throughout the coating indicates that 12% of the Ag has diffused out of the matrix during the 20 min anneal. Additionally, we note that the rapid diffusion in the case of no cap layer or through the cap layer for $E_i = 30$ eV, in combination with the lack of diffusion through the cap layer for $E_i = 150$ eV, indicates that Ag transport likely occurs through nanoporous boundaries within the film, rather than by conventional bulk or grain boundary diffusion. Open nanoporous boundaries provide high-diffusivity pathways for Ag to diffuse, akin to diffusion along a free surface. Generally, the diffusivity D_s along a free surface is larger than the diffusivity D_b along grain boundaries, which is in turn larger than the diffusivity D_l through the lattice. That is, $D_s > D_b > D_l$ [33].

3.2. High temperature tribological response

In this section, the high-temperature self-lubricating properties of CrN–Ag composite coatings with a dense CrN cap layer ($E_i = 150$ eV) are compared to the properties of an identical CrN–Ag composite coating without cap layer and also with a pure CrN coating. Prior research [13] has demonstrated that the key parameter determining lubricant transport and, in turn, tribological response of the composite films is the difference between growth temperature T_s and testing temperature

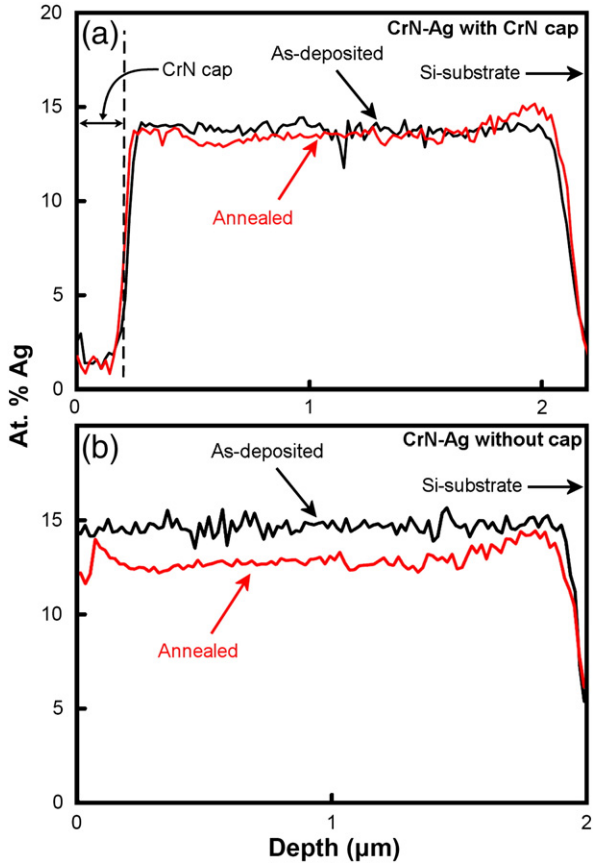

Fig. 2. Auger depth profiles of CrN–Ag nanocomposites deposited on Si (a) with a 200 nm thick pure CrN cap layer and (b) without a cap layer. Profiles are plotted for both the as-deposited coatings as well as after annealing at $T_a = 625$ °C for 20 min.

T_t, or $\Delta T = T_t - T_s$. In this case, the coatings were investigated by sliding tests against 6 mm diameter alumina balls at a test temperature $T_t = 550$ °C, which corresponds to a $\Delta T = +50$ °C, which is expected to yield considerable lubricant transport within the composite in the absence of a diffusion barrier [13]. Fig. 3 shows plots of the friction coefficient μ versus cycle number, with 0.016 m/cycle, for the three sample architectures. The friction coefficient for pure CrN remains relatively stable at $\mu = 0.41 \pm 0.02$ for the entire test, indicating little change in the sliding surface over the 10,000 cycles. The stated

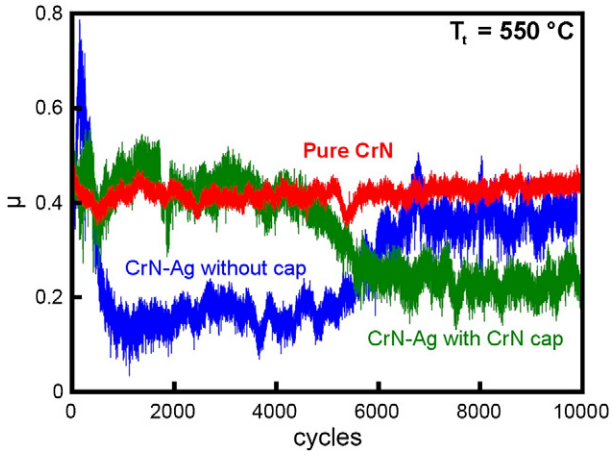

Fig. 3. Friction coefficient μ versus number of cycles during ball-on-disk testing against alumina at $T_t = 550$ °C, for a pure CrN coating, a CrN–Ag coating, and a CrN–Ag coating with a dense CrN cap layer deposited with $E_i = 150$ V.

uncertainty of 0.02 corresponds to one standard deviation of the measured instantaneous μ-value. The composite without cap layer exhibits an initially high $\mu \approx 0.6$ which drops to a transient minimum where μ remains constant at 0.16 ± 0.03 for ~5000 cycles, prior to increasing up to $\mu = 0.39 \pm 0.04$. The initially high friction is attributed to the presence of irregular Ag mounds that have formed at the surface during the 30 min thermal soak prior to testing, while the transient minimum in μ is due to a lubricious bearing layer, likely composed of Ag along with Cr oxides (Cr_2O_3, Cr_3O_4) and mixed oxides such as $AgCrO_2$ [15], that is continuously replenished by Ag moving from the matrix to the sliding surface. However, as testing proceeds, the amount of mobile Ag within the composite matrix decreases which, in turn, leads to a decreasing lubricant flux to the surface. Therefore, at some point, the Ag wear rate exceeds the lubricant flux so that the lubricious surface layer is insufficiently replenished, leading to the observed increase in μ after ~5000 cycles. In contrast, the CrN–Ag composite coating with a CrN cap layer exhibits a $\mu = 0.43 \pm 0.04$ for the initial 4500 cycles, followed by a gradual decrease over the next 1500 cycles to a value of 0.23 ± 0.03 for cycle 6000–10,000. The initial friction coefficient is comparable to that for pure CrN, indicating that the pure CrN cap layer initially dominates the tribological properties. The decrease in μ from cycle 4500–6000 is attributed to the gradual development of wear mediated openings in the cap layer which allow Ag transport from the composite through the cap to the sliding surface, as evidenced by the subsequent SEM analyses. Thus, Ag lubrication becomes effective for cycles >6000 when the diffusion barrier is sufficiently degraded to allow lubricant flow to the surface. This behavior represents adaptive lubrication, since Ag lubrication is only initiated when wear of the barrier cap layer indicates an actual need for lubrication. In addition, the opposite trend observed for the uncapped versus the capped nanocomposite coatings indicates the versatility of these structures and demonstrates the potential of this materials system for designing coating architectures that perform optimally for specific operating conditions.

Fig. 4(a) and (b) are surface profilometry images after high-temperature tribological testing, showing the wear track of the uncapped and capped CrN–Ag coatings, respectively. The uncapped surface in (a) exhibits a track which is deeper and shows considerably more wear debris next to the track than the capped coating in (b). This difference is quantified by the cumulative wear rate which is 10.2×10^{-6} mm^3/Nm for the uncapped composite and 3.1×10^{-6} mm^3/Nm for the capped coating. Here we note that these stated wear rates are for the entire 10,000 cycle tests, that is, they include for (a) both the low-friction regime where Ag solid lubrication is active and the higher friction regime where Ag has been depleted, and for (b) the initial high-friction regime where the cap layer has not been fully penetrated and the low-friction regime where the reduction in μ is attributed to the flux of Ag to the surface through the worn cap layer. The corresponding wear rate for a pure CrN coating is 11.1×10^{-6} mm^3/Nm, similar to the value for the uncapped composite. That is, the capped composite coating is clearly the most wear resistant, having a 3.3 and 3.6 times lower wear rate than the uncapped composite and the pure CrN coatings, respectively.

SEM and EDS surface analyses were performed after tribological testing in order to gain additional insight into the different friction and wear behavior of the uncapped and capped coatings. The wear track of the uncapped CrN–Ag composite is shown in the SEM micrograph in Fig. 5(a). It has a measured Ag concentration within the track of 11.1 at.%, which is just half of the average concentration (22 at.%) prior to tribological testing, indicating that a significant fraction of the solid lubricant has moved out of the matrix and been worn away during high-temperature sliding. While there is minimal wear of the alumina counterface, the mechanism of wear of the composites is likely a mix of adhesive wear, with deformation and some transfer of the ductile Ag to the alumina counterface as described in prior work [13], and abrasive wear associated with sliding of CrN and oxide based wear debris. The reduced Ag concentration measured within the wear track supports the above interpretation of the μ versus cycle data in Fig. 3, showing that the

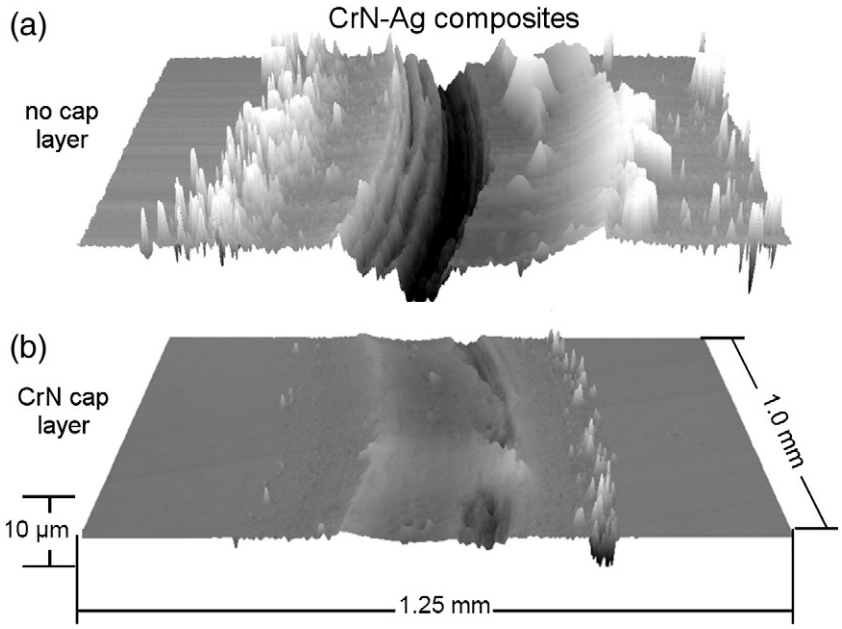

Fig. 4. 3-D surface profiles of CrN–Ag composite coatings after tribological testing (a) without and (b) with a cap layer.

uncapped coating is in a low-lubrication state at the end of the sliding test, consistent with the depleted solid lubricant in the wear track. The larger magnification micrograph in the inset of Fig. 5(a) from the uncapped surface which has not been in contact with the counterface (i.e. outside the wear track), shows Ag agglomerates that developed during high-temperature testing, confirming that the Ag moves readily through the nanocomposite during testing at 550 °C. Fig. 5(b) shows the wear track of the capped composite coating. In contrast to the uncapped coating, the average Ag concentration within the wear track for the capped coating is 42 at.%. This is nearly twice the original Ag concentration, indicating an Ag enriched surface layer, which is attributed to Ag flux to the surface during testing. The higher magnification micrograph (middle right) shows the edge of the Ag bearing layer that has been sheared by direct contact with the alumina

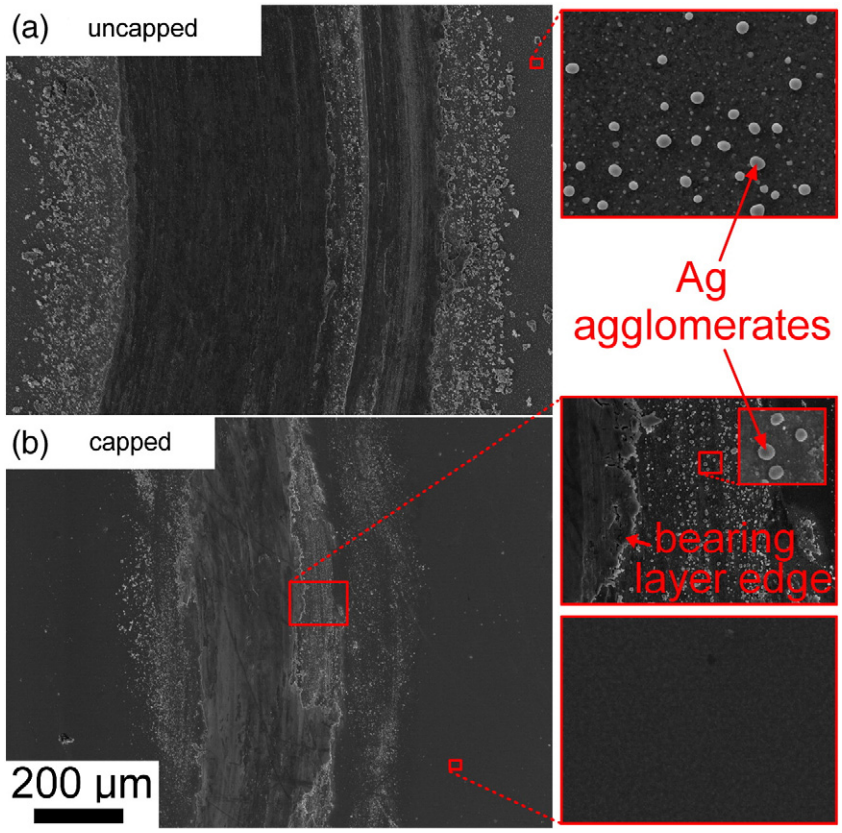

Fig. 5. Plan-view SEM micrographs of wear tracks for (a) uncapped and (b) capped coatings. The images on the right are higher magnification views of the outlined areas.

ball counterface. The presence of unsheared Ag agglomerates directly to the right of the bearing layer edge indicates that at some point during sliding the cap layer has worn through in this region, allowing Ag to diffuse to the surface, however, the flux of Ag to the surface within the wear track leaves the area protected from further direct contact with the alumina ball. This lends support to the interpretation of the μ versus cycle data, wherein the friction drop for this sample is attributed to Ag diffusing through wear mediated openings in the cap layer. The higher magnification micrograph from an area outside the wear track (bottom right) indicates no Ag agglomerates, confirming that the dense cap layer effectively acts as a lubricant diffusion barrier if it is not worn away by substantial sliding contact.

4. Conclusions

CrN–Ag composite films were deposited with 22 at.% Ag concentration both with and without a cap layer. CrN cap layers of 200 nm thickness were deposited onto the composites *in-situ* with either a −30 V floating potential or with a −150 V substrate bias. Ion irradiation due to the bias results in a dense cap layer that acts as an effective diffusion barrier for Ag, as determined by vacuum annealing experiments. Tribological testing at a temperature where Ag is mobile within the composite shows distinctly different friction traces for the uncapped versus the capped coatings: For the uncapped coating, Ag diffuses to the surface and effectively lubricates, however, the Ag is depleted during the sliding test due to uncontrolled lubricant transport. In contrast, Ag flux for the capped coating occurs only within the wear track and forms a lubricious bearing layer that yields low friction and a 3.3× lower cumulative wear rate over the 10,000 cycle test.

Acknowledgments

This research was supported by the United States Army TEX3 Program, through the Armament Research, Development and Engineering Center (ARDEC), and by the National Science Foundation under grant Nos. CMMI-0653843 and DMR-0645312.

References

[1] C. Donnet, A. Erdemir, Surf. Coat. Technol. 180–181 (2004) 76.
[2] A.A. Voevodin, J.S. Zabinski, C. Muratore, Tsinghua Sci. Technol. 10 (2005) 665.
[3] S.M. Aouadi, B. Luster, P. Kohli, C. Muratore, A.A. Voevodin, Surf. Coat. Technol. 204 (2009) 962.
[4] C. Muratore, A.A. Voevodin, Annu. Rev. Mater. Res. 39 (2009) 297.
[5] H.A. Jehn, Surf. Coat. Technol. 131 (2000) 433.
[6] W. Wang, Surf. Coat. Technol. 177–178 (2004) 12.
[7] A.A. Voevodin, J.P. O'Neill, J.S. Zabinski, Surf. Coat. Technol. 116–119 (1999) 36.
[8] C. DellaCorte, R.J. Bruckner, Oil-Free Rotor Support Technologies for an Optimized Helicopter Propulsion System, June 2007, NASA TM 214845.
[9] M.J. Valco, C. DellaCorte, Emerging Oil-Free Turbomachinery Technology for Military Propulsion and Power Applications, Proceedings of the 23rd Army Science Conference, Orlando, FL, December 2002.
[10] V. Derflinger, H. Brandle, H. Zimmermann, Surf. Coat. Technol. 113 (1999) 286.
[11] S.J. Shaffer, M.J. Rogers, Wear 263 (2007) 1281.
[12] C. Muratore, J.J. Hu, A.A. Voevodin, Surf. Coat. Technol. 203 (2009) 957.
[13] C.P. Mulligan, T.A. Blanchet, D. Gall, Wear 269 (2010) 125.
[14] H. Kostenbauer, G.A. Fontalvo, C. Mitterer, J. Keckes, Tribol. Lett. 30 (2008) 53.
[15] K. Kutschej, C. Mitterer, C.P. Mulligan, D. Gall, Adv. Eng. Mater. 8 (2006) 1125.
[16] J.J. Hu, C. Muratore, A.A. Voevodin, Composites Sci. Technol. 67 (2007) 336.
[17] S.M. Aouadi, Y. Paudel, W.J. Simonson, Q. Ge, P. Kohli, C. Muratore, A.A. Voevodin, Surf. Coat. Technol. 203 (2009) 1304.
[18] C. Muratore, A.A. Voevodin, J.J. Hu, J.S. Zabinski, Wear 261 (2006) 797.
[19] C. Muratore, J.J. Hu, A.A. Voevodin, Thin Solid Films 515 (2007) 3638.
[20] A.A. Voevodin, J.J. Hu, J.G. Jones, T.A. Fitz, J.S. Zabinski, Thin Solid Films 401 (2001) 187.
[21] P. Basnyat, B. Luster, Z. Kertzman, S. Stadler, P. Kohli, S. Aouadi, J. Xu, S.R. Mishra, O.L. Eryilmaz, A. Erdemir, Surf. Coat. Technol. 202 (2007) 1011.
[22] S.M. Aouadi, A. Bohnhoff, M. Sodergren, D. Mihut, S.L. Rohde, J. Xu, S.R. Mishra, Surf. Coat. Technol. 201 (2006) 418.
[23] C.P. Mulligan, D. Gall, Surf. Surf. Coat. Technol. 200 (2005) 1495.
[24] C.P. Mulligan, T.A. Blanchet, D. Gall, Surf. Coat. Technol. 203 (2008) 584.
[25] L.I. Maissel, P.M. Schaible, J. App. Phys. 36 (1964) 237.
[26] D.M. Mattox, G.J. Kominiak, J. Vac. Sci. Technol. 9 (1971) 528.
[27] J.E. Greene, S.A. Barnett, J. Vac. Sci. Technol. 21 (1982) 285.
[28] D. Gall, C.-S. Shin, T. Spila, M. Odén, M.J.H. Senna, J.E. Greene, I. Petrov, J. App. Phys. 91 (2002) 3589.
[29] R.G. Munro, J. Am. Ceram. Soc. 80 (1997) 1919.
[30] D. Gall, I. Petrov, N. Hellgren, L. Hultman, J.-E. Sundgren, J.E. Greene, J. Appl. Phys. 84 (1998) 6034.
[31] L. Hultman, S.A. Barnett, J.E. Sundgren, J.E. Greene, J. Cryst. Growth 92 (1988) 639.
[32] H.L. Marcus, "Auger Electron Spectroscopy", in Encyclopedia of Materials, Sci. Technol. (2008) 393.
[33] D.A. Porter, K.E. Easterling, Phase Transformations in Metals and Alloys, 2nd ed., Chapman & Hall, London, UK, 1992, p. 98.